Published online 12 January 2009 *Nucleic Acids Research, 2009, Vol. 37, No. 5* ***1541–1554***
doi:10.1093/nar/gkn1081

The effect of the TRF2 N-terminal and TRFH regions on telomeric G-quadruplex structures

Ilene M. Pedroso, William Hayward and Terace M. Fletcher*

Department of Biochemistry and Molecular Biology, University of Miami Miller School of Medicine, Miami, FL 33101-6129, USA

Received September 16, 2008; Revised December 20, 2008; Accepted December 23, 2008

ABSTRACT

The sequence of human telomeric DNA consists of tandem repeats of 5′-d(TTAGGG)-3′. This guanine-rich DNA can form G-quadruplex secondary structures which may affect telomere maintenance. A current model for telomere protection by the telomere-binding protein, TRF2, involves the formation of a t-loop which is stabilized by a strand invasion-like reaction. This type of reaction may be affected by G-quadruplex structures. We analyzed the influence of the arginine-rich, TRF2 N-terminus ($TRF2^{B}$), as well as this region plus the TRFH domain of TRF2 ($TRF2^{BH}$), on the structure of G-quadruplexes. Circular dichroism results suggest that oligonucleotides with 4, 7 and 8 5′-d(TTAGGG)-3′ repeats form hybrid structures, a mix of parallel/antiparallel strand orientation, in K^+. $TRF2^{B}$ stimulated the formation of parallel-stranded structures and, in some cases, intermolecular structures. $TRF2^{BH}$ also stimulated intermolecular but not parallel-stranded structures. Only full-length TRF2 and $TRF2^{BH}$ stimulated uptake of a telomeric single-stranded oligonucleotide into a plasmid containing telomeric DNA in the presence of K^+. The results in this study suggest that G-quadruplex formation inhibits oligonucleotide uptake into the plasmid, but the inhibition can be overcome by TRF2. This study is the first analysis of the effects of TRF2 domains on G-quadruplex structures and has implications for the role of G-quadruplexes and TRF2 in the formation of t-loops.

INTRODUCTION

Telomeres are chromatin structures located at the ends of chromosomes that function to protect genomic integrity. Disruption of this nucleoprotein complex elicits DNA damage signaling, resulting in apoptosis or senescence (1). The telomeres in normal somatic cells also function as mitotic clocks by shortening with each round of replication that precedes cell division, or they shorten as a result of oxidative damage (2). Once telomeres reach a critical minimum length, cells exit the cell cycle. This process is known as replicative senescence and can be bypassed by upregulation of the telomere-specific reverse transcriptase, telomerase (3).

The sequence of mammalian telomeric DNA is composed of several kilobase pairs of tandem repeats of TT AGGG. This double-strand region is followed by a 3′ overhang of the TTAGGG sequence. Bound to this chromosomal region is a telomere-specific protein complex, known as shelterin, which maintains telomere length and protects telomeres from being mistaken as damaged DNA (1). Thus far, six proteins are known to be in the shelterin complex. Some of these bind directly to DNA and all are connected to each other via protein–protein interactions of various adaptor proteins. Two proteins, called TTAGGG Repeat Factors 1 and 2 (TRF1 and TRF2), bind to double-stranded telomeric DNA through myb/SANT DNA-binding domains (4–6). Another protein, Protection of Telomeres 1 (POT1), interacts directly with telomeric single-stranded DNA (7). Disruption of this complex by dominant-negative TRF2 mutants results in chromosome end-to-end fusions, loss of the G-strand overhang, and ATM/p53 activation, leading to apoptosis or senescence (8,9).

In addition to the nucleoprotein complex, the current model for telomere protection involves topological remodeling of DNA architecture into looped structures called t-loops (10). These telomeric DNA higher-order structures have been isolated from cells after psoralen crosslinking. The ability of *Esherichia coli* single-strand-binding protein to bind to the junction of the loop suggests the presence of some form of single-stranded or other non-duplex DNA structures (10). TRF2 was able to stimulate the formation of t-loops *in vitro*, partly through its ability to oligomerize through its TRF homology (TRFH) domain (11) and

*To whom correspondence should be addressed. Tel: +1 305 243 6297; Fax: +1 305 243 3955; Email: tfletcher@med.miami.edu

possibly via a structurally uncharacterized linker region (12). In addition to interacting with double-stranded telomeric DNA, TRF2 interacts with other DNA motifs such as three-way, four-way (13) and single-strand/double-strand DNA junctions (12). Binding to these structures is likely to involve a glycine/arginine-rich region in the N-terminus (13). This secondary DNA-binding activity may increase t-loop formation that involves the end of the duplex telomeric DNA and the G-strand overhang (14,15). A truncation mutant lacking this region results in loss of telomeres, most likely through a recombination mechanism (16). A third activity found in TRF2 is the ability to stimulate the uptake of a single-stranded telomeric oligonucleotide into a plasmid containing telomeric DNA (17). This is consistent with the t-loop model for TRF2 protection of telomeric ends, which involves looping of the telomere and some kind of strand invasion of the G-strand overhang into the double-stranded region of the telomere.

Minimally considered is how other secondary structures, known to occur with guanine-rich DNA sequences, affect the activities of TRF2. Guanine-rich DNA has been shown to form highly stable, G-quadruplex structures in physiological concentrations of Na^+ and K^+ (18). These DNA structures are built upon the G-tetrad structural motif in which four guanines are in a planar arrangement and are stabilized by Hoogsteen-like hydrogen bonding and a cation chelated by the keto oxygen of the guanines (Figure 1F). A variety of G-quadruplexes can form on human telomeric DNA sequence and the type can be modulated by type of cation, cation and DNA concentration, number of TTAGGG repeats, and reaction time (18).

G-quadruplexes can inhibit important activities associated with telomere maintenance. These structures have been shown to affect telomerase activity *in vitro* (19–21). Moreover, specific types of G-quadruplexes can have differential effects on certain activities. For example, an antiparallel, intramolecular G-quadruplex inhibits *Tetrahymena* and *Oxytricha* telomerase activity whereas a parallel, intermolecular structure is a suitable substrate (22,23). In addition, G-quadruplex-stabilizing small molecules can accelerate telomere shortening (24), reduce the G-strand overhang (25) and disrupt the telomere nucleoprotein complex, as judged by loss of POT1 (24,26) and TRF2 (27) from the ends. This is consistent with the finding that formation of a G-quadruplex in the G-strand overhang at a model telomeric end can inhibit recruitment of TRF2/POT1-containing complexes from HeLa cell crude extracts (28). However, the quadruplex structure does not inhibit binding of purified TRF2 (12).

The described results suggest that TRF2 functions to stabilize a looped protective structure that may involve the G-strand overhang. However, the G-strand overhang also has the potential to form G-quadruplex structures. If TRF2 is capable of interacting with different types of DNA structures, and its affinity is stimulated by the presence of a G-strand overhang at telomeric ss/ds DNA junctions, how might TRF2 affect the formation and conformation of potential G-quadruplex structures within the overhang? In addition, how do TRF2 and G-quadruplex structures affect the formation of t-loops?

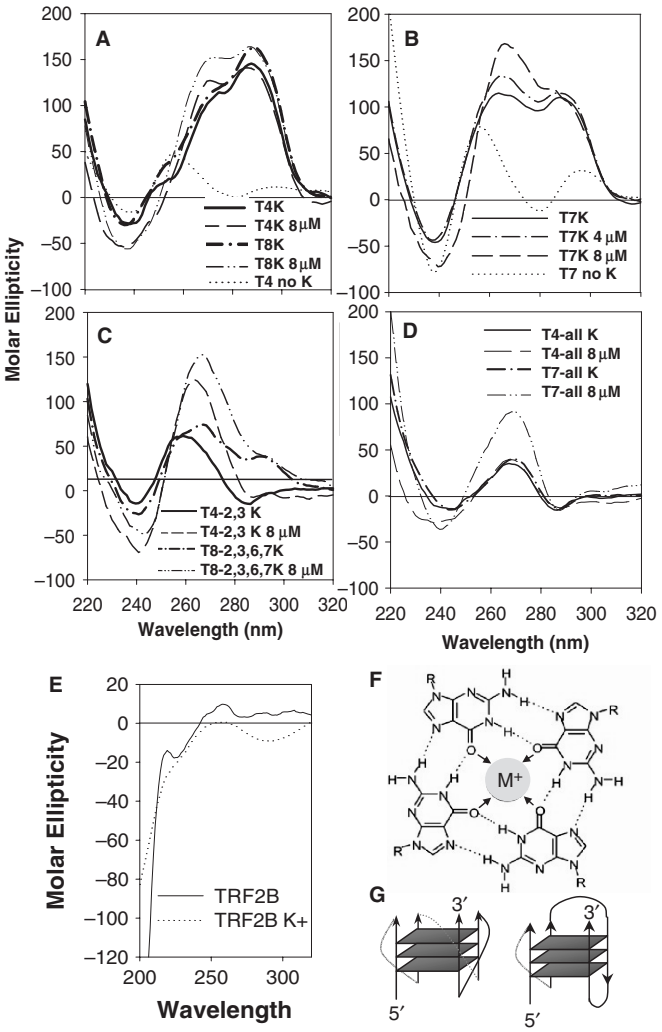

Figure 1. CD spectra of $TRF2^B$ with 4 μM telomeric oligonucleotides [T*n* = $(TTAGGG)_n$ or T*n*-X, where X indicates which repeats in the 5′3′ direction have been altered to 5′-(TTAGAG)-3′] in 15 mM Na_2PO_4 and 100 mM KCl (**A**–**D**). The 'No K' spectra in A and B obtained in 1 mM Na_2PO_4 alone to illustrate the spectra of non-G-quadruplex structures. The 4 or 8 μM refer to the amount of $TRF2^B$ added to the DNA at 5 min after heating to 95°C and transferring to room temperature. Samples remained at room temperature for 24 h before spectra were obtained. Molar ellipticity is in deg cm^2/dmol of bases. CD spectra of 4 μM TRF2B alone, with or without 100 mM KCl, as indicated (**E**). Molar ellipticity is in deg cm^2/dmol of amino-acid residues. Structure of the G-tetrad coordinating to a metal (M^+) cation (**F**). Examples of intramolecular G-quadruplexes formed by T4 with parallel (left) or hybrid-type parallel/antiparallel (right) strand orientation (**G**).

To address these questions, we analyzed the structures of G-quadruplexes in the presence of the glycine/arginine-rich, N-terminus of TRF2 ($TRF2^B$). We found that this region of the protein stimulated the formation of parallel-stranded, intermolecular structures as judged by circular dichroism (CD) and native polyacrylamide gels. Interestingly, in the presence of K^+, $TRF2^B$ induced parallel-stranded structures on oligonucleotides previously shown to form hybrid G-quadruplexes comprised of both parallel and antiparallel strand orientations.

However, $TRF2^{B}$ did not induce parallel-stranded structures in Na^{+}. Uptake of a single-stranded telomeric, 5′-d(TTAGGG)$_7$-3′ oligonucleotide by plasmids containing telomeric DNA was stimulated by Mg^{2+} and/or Na^{+} but slightly inhibited by higher concentrations of K^{+}. $TRF2^{B}$ further stimulated oligonucleotide uptake in the presence of Na^{+} but not in K^{+}. However, low concentrations of full-length TRF2 and a TRF2 construct containing both the N-terminus and the TRFH domain ($TRF2^{BH}$) were able to stimulate oligonucleotide uptake even in the presence of K^{+}. Furthermore, $TRF2^{BH}$ did not induce the formation of parallel-stranded G-quadruplexes. These data are the first to implicate TRF2 as a G-quadruplex modulator. However, G-quadruplexes may only weakly affect TRF2-dependent, t-loop formation unless other factors, such as molecular crowding, come into play.

MATERIALS AND METHODS

Telomeric DNA oligonucleotides

Oligonucleotides of telomeric repeats were purchased from Sigma Genosys. Telomeric sequences (T*n*) had 4, 7 and 8, 5′-d(TTAGGG)-3′ repeats (T4, T7 and T8) as described in Table 1. Other oligonucleotides (T*n*-X) had some or all of the repeats altered to 5′-d(TTAGAG)-3′. The -X denotes which repeats in the 5′ to 3′ direction were altered. Therefore, T4-2,3 refers to the sequence 5′-d(TTAGGGTTAGAGTTAGAGTTAGGG)-3′, while T8-2,3,6,7 refers to 5′-d(TTAGGGTTAGAGTTAGAGTTAGGGTTAGGGTTAGAGTTAGAGTTAGGG)-3′, and T4-all is 5′-d(TTAGAGTTAGAGTTAGAGTTAGAG)-3′.

$TRF2^{B}$, $TRF2^{BH}$, TRF2 constructs, expression and purification

The basic N-terminal region of TRF2 ($TRF2^{B}$), containing amino acids 2–31 and an N-terminal biotin followed by a lysine (Biotin-KAGGGGSSDGSGRAAGRRASRSSGRARRGRH) was synthesized by Invitrogen. The $TRF2^{BH}$ (amino acids 3–247) was constructed by GenScript Corporation with optimized codons and cloned into the NdeI/BamHI sites of pET15b for expression in *E. coli* BL21 cells (Invitrogen). The 6× His-tagged protein was purified by HisTrap FF Ni^{2+}–Sepharose 6 and HiPrep 26/10 chromatography. Full-length TRF2 was baculovirus-expressed in Sf9 cells and purified as described previously (12).

Circular Dichroism with $TRF2^{B}$ and $TRF2^{BH}$

Samples were prepared with 4 μM telomeric oligonucleotide (Table 1) in Na_2PO_4 (1 or 15 mM) and KCl (0 or 100 mM). Reactions were heated for 5 min at 95°C and immediately transferred to room temperature to cool for 5 min before the addition of 8 μM $TRF2^{B}$ (unless otherwise specified) or an equal volume of H_2O. Spectra at wavelengths 200–320 nm were obtained with a Jasco J-720 spectropolarimeter in 200 μl cells with a 0.1 cm path length. The resulting CD spectra were the average of 10 consecutively measured scans taken in 0.5 nm increments over 25 min.

To analyze the CD spectrum of $TRF2^{BH}$ with or without oligonucleotides, samples were prepared with or without 2 μM oligonucleotide and 100 mM KF in 1 mM Na_2PO_4. In addition, the $TRF2^{BH}$ buffer contributed 12.5 mM NaCl to the reaction. Reactions were heated for 5 min at 95°C then transferred room temperature to cool for 5 min before the addition of $TRF2^{BH}$ or an equal volume of $TRF2^{BH}$ buffer. Reactions were incubated at room temperature for 1, 4, 8 or 24 h after the addition of $TRF2^{BH}$. CD spectra at wavelengths 190–320 nm were obtained at room temperature with a Jasco J-720 spectropolarimeter in 200 μl cells with a 0.1 cm path length. The resulting CD spectra were the average of 10 consecutively measured scans taken in 0.5 nm increments over 25 min.

Native polyacrylamide gel electrophoresis

Reactions with $TRF2^{B}$ (20 μl final) were prepared similarly to CD experiments with 4 μM 5′-[^{32}P]-labeled oligonucleotides in 100 mM KCl and 1 or 13.5 mM Na_2PO_4. Samples were heated for 5 min at 95°C and cooled for 5 min to room temperature. An equal volume of the appropriate $TRF2^{B}$ stock was added to each reaction to reach final concentrations of 0, 2, 4, 8 and 16 μM. Reactions were left for 24 h at room temperature before the addition of bromophenol blue/xylene cyanol loading dye. Samples were loaded onto 8% (29:1, acrylamide:*bis*-acrylamide) native polyacrylamide gels prepared in 1× TTE (40 mM Tris–taurine pH 8.0, 10 mM EDTA), 15 mM Na_2PO_4 and 100 mM KCl. Electrophoresis was carried out in a 4°C room at 3 V/cm for 16–20 h. Gels were dried and a Storm 840 Phosphorimager (Molecular Dynamics) was used for band detection. Band migration and intensities were determined using ImageQuant 5.2 software.

Reactions with $TRF2^{BH}$ (20 μl final) were prepared in 100 mM KCl, 22.5 mM NaCl, 1XTE (10 mM Tris pH 8.0, 1 mM Na_2EDTA) with 50 nM or 4 μM 5′-[^{32}P]-labeled

Table 1. Telomeric oligonucleotide sequences

	5′→3′ Sequence
T4	TTAGGG TTAGGG TTAGGG TTAGGG
T4-2,3	TTAGGG TTAGAG TTAGAG TTAGGG
T7	TTAGGG TTAGGG TTAGGG TTAGGG TTAGGG TTAGGG TTAGGG
T8	TTAGGG TTAGGG TTAGGG TTAGGG TTAGGG TTAGGG TTAGGG TTAGGG
T8-2,3,6,7	TTAGGG TTAGAG TTAGAG TTAGGG TTAGGG TTAGAG TTAGAG TTAGGG
T*n*-all	(TTAGAG)*n*

oligonucleotides. Samples were then heated for 5 min at 95°C and cooled on ice for 1 min. An equal volume of $TRF2^{BH}$ was added to each reaction to reach final concentrations of 0, 0.5, 1, 2 and 4 μM. Reactions were left for 8 or 24 h at room temperature before the addition of bromophenol blue/xylene cyanol loading dye. Samples were loaded onto 12% (29:1) native polyacrylamide gels prepared in 0.5× TTE (40 mM Tris–taurine pH 8.0, 10 mM EDTA) and 50 mM KCl. Electrophoresis was carried out in a 4°C room at 6.5 V/cm for ~8 h. Gels were dried and a Storm 840 Phosphorimager (Molecular Dynamics) was used for band detection. Band migration and intensities were determined using ImageQuant 5.2 software.

Plasmid uptake of single-stranded oligonucleotides

Uptake of telomeric oligonucleotides by a plasmid containing telomeric sequences was analyzed using T7 or T4 (data not shown) and pRST5 plasmid containing ~96 TTAGGG repeats [provided by Jack D. Griffith (14)]. Sample buffers containing 50 mM HEPES pH 7.9, 0.1 mg/ml BSA, 1 mM DTT, 2% glycerol were prepared with 0–400 mM KCl or NaCl, and 0–20 mM $MgCl_2$ as indicated. pRST5 (20 ng/μl) and indicated concentrations of $TRF2^{B}$ or $TRF2^{BH}$ were preincubated in reaction buffer for 15 min at room temperature. Meanwhile, 5′-[^{32}P]-labeled T7 was heated for 5 min at 95°C, cooled on ice 1 min then added to reaction to make a final concentration of 50 nM. Alternatively, T7 was heated and preincubated overnight in the sample buffer before the addition of pRST5 and $TRF2^{B}$ or $TRF2^{BH}$. Reactions (10 μl) were incubated at room temperature for 15 min or overnight before the reaction was stopped by SDS (1% final) and 6 μg of proteinase K. Bromophenol blue/xylene cyanol loading dye was added and samples were electrophoresed on 1% agarose, 0.5× TBE gels in the cold room for 2 h at 4 V/cm. Initial gels were stained in SYBR gold to ensure even amounts of pRST5 in each lane (data not shown). Samples were also electrophoresed in 15% native polyacrylamide gels with 100 mM KCl to detect intermolecular G-quadruplexes (data not shown). Gels were dried and a Storm 840 Phosphorimager (Molecular Dynamics) was used for band detection. Band migration and intensities were determined using ImageQuant 5.2 software.

Watson–Crick duplex annealing assay

Reactions with 5′-[^{32}P]-labeled T7 or T7-all (2.2 nM, 10 μl total reaction) were either heated at 95°C in the presence of indicated salts for 5 min, then slowly cooled to room temperature over an hour, or heated and transferred immediately to room temperature, followed by addition of $TRF2^{B}$ and incubated for 24 h. One microliter of C7 or C7-all complementary strand stocks were added to the G-strand to reach the final concentrations of salt and oligonucleotides as indicated in Figure 6. Annealing reactions were incubated at room temperature for 15 min, 16 h or 40 h before electrophoresis on a 12% (29:1) native polyacrylamide gel prepared in 0.5× TBE and indicated salts. Electrophoresis was carried out in a 4°C room at 12.5 V/cm for 1 h. Gels were dried and a Storm 840 Phosphorimager (Molecular Dynamics) was used for band detection. Band migration and intensities were determined using ImageQuant 5.2 software.

RESULTS

TRF2 is known to interact with telomeric DNA, and this interaction was found to respond to the length and structure of the 3′-G-strand overhang (12). While the myb/SANT domain binds to the double-strand telomeric region (6), the basic N-terminal domain of TRF2 may be responsible for interacting with the single-strand DNA. The basic, N-terminal region of TRF2 ($TRF2^{B}$) has eight arginines. Consequently, we predicted that this region of the protein could influence the formation of certain G-quadruplex structures in a manner similar to other polycations such as putrescine, polylysine and the beta subunit of the Oxytricha TEBP (29,30). While $TRF2^{B}$ is positively charged and may neutralize charges on the DNA, the adjacent TRFH domain, mediates TRF2 homodimerization (11). The two domains together ($TRF2^{BH}$) may facilitate intermolecular structure formation on DNA bound to TRF2. We previously found that the type of G-quadruplex structure formed by human telomeric DNA is highly sensitive to oligonucleotide concentration, sequence and reaction time (31). We used the information gained by our previous work to select oligonucleotides with which to study the effect of the $TRF2^{B}$ and $TRF2^{BH}$ on G-quadruplex secondary structures.

To investigate the role of DNA length on secondary structure formation, oligonucleotides T4, T7 and T8, denoting 4, 7 and 8 5′-d(TTAGGG)-3′ repeats respectively, were synthesized (Table 1). Additionally, because the central guanine is believed to be important for G-quadruplex stability, the oligonucleotides had some of the 5′-d(TTAG GG)-3′ repeats altered to 5′-d(TTAGAG)-3′. For example, T4-2,3 had four telomeric repeats but the second and third repeats were converted to 5′-d(TTAGAG)-3′ and T4-all had all four repeats altered to 5′-d(TTAGAG)-3′. These oligonucleotides were used to study position effects of sequence alterations on G-quadruplex formation. The structures formed on these oligonucleotides in Na^+ and K^+, under various conditions, were characterized using native polyacrylamide gel electrophoresis and CD spectroscopy.

TRF2 N-terminal peptide ($TRF2^{B}$) stimulates the formation of parallel-stranded structures in K^+

CD was used to analyze the structures of oligonucleotides T4 [5′-d$(TTAGGG)_4$-3′] and T8 [5′-d$(TTAGGG)_8$-3′]. As previously observed, these oligonucleotides have spectra in 100 mM K^+ with a large positive signal near 290 nm, a shoulder around 270 nm and a small negative ellipticity near 240 nm, which together are characteristic of hybrid-type G-quadruplex structures (Figure 1G) composed of a combination of parallel and antiparallel strand orientation (32–37). The addition of 8 μM $TRF2^{B}$ to 4 μM of either T4 or T8 resulted in an increase in the positive ellipticity centering around 265 nm (Figure 1A). These changes were not due to contributions of $TRF2^{B}$ alone to the spectrum

since relatively little detectable signals in that region were obtained with TRF2^B alone (Figure 1E). Considering that this type of spectrum for telomeric sequences is usually indicative of glycosidic bonds being in the *anti* conformation, the most likely explanation is that TRF2^B increased the presence of parallel-stranded G-quadruplexes (Figure 1G). However, other structures with these distinct spectra cannot be ruled out at this time.

We previously (31) observed that T7 [5′-d(TTAGGG)$_7$-3′] was capable of forming a structure with both parallel/antiparallel strand orientation in K^+ when heated and cooled quickly by transferring directly to room temperature. The spectrum was similar to those of T4 and T8 in that it had a positive peak at 290 nm and a negative at 240 nm. A broad shoulder centering around 255–260 also appeared under these conditions (31). This spectrum was also observed in 15 mM Na_2PO_4, 100 mM K^+ (Figure 1B). Interestingly, the addition of 4 μM TRF2^B resulted in an increase in the positive signal at 265 nm (Figure 1B). This is similar to the spectrum achieved by heating and then slowly cooling the T7 oligonucleotide over several hours, and coincided with the formation of an intermolecular structure (Figure 4) (31). Furthermore, the addition of 8 μM TRF2^B induced a significant increase of the signal at 265 nm, with the signal at 290 nm being a shoulder by comparison, suggesting the presence of relatively more parallel-stranded structures in the T7 mixture than observed with T4 or T8.

Previous studies showed that the alteration of the central two 5′-d(TTAGGG)-3′ to 5′-d(TTAGAG)-3′ within a stretch of four repeats (T4-2,3) resulted in a disruption of the intramolecular, parallel/antiparallel-stranded G-quadruplex (31). Instead, parallel-stranded, intermolecular G-quadruplexes formed when samples were heated and cooled slowly to room temperature. These structures did not form under rapid cooling conditions (Figures 1C and 4). Thus, the spectra of T4-2,3 and T8-2,3,6,7 in 15 mM Na_2PO_4, 100 mM K^+ did not show evidence of G-quadruplex formation and resembled the spectra in 1–15 mM Na_2PO_4 alone (data not shown). However, addition of TRF2^B to either oligonucleotide resulted in a spectrum with a strong positive peak near 265 nm (Figure 1C). In the presence of TRF2^B, the T4-2,3 spectrum had no peak at 290 nm and the shoulder at 290 nm for T8-2,3,6,7 was relatively weak when compared to that at 265 nm. These spectra are suggestive of parallel-stranded structures. The results also demonstrate that TRF2^B stimulated the formation of these structures under conditions in which they otherwise would not form.

We previously demonstrated that alteration of all 5′-d(TTAGGG)-3′ repeats to 5′-d(TTAGAG)-3′ (Tn-all) abolished the ability to form G-quadruplex structures in K^+ (31). The spectra of T4-all and T7-all show small negative peaks near 240 nm and 280 nm, and small positive peaks between 265 nm and 270 nm (Figure 1D). The addition of the TRF2^B did not change the spectrum of T4-all (Figure 1D). However, the spectrum for T7-all with TRF2^B exhibited a slight increase in intensity at ~270 nm. This spectrum has some similarity to those observed for T7-all and T8-all in Sr^{2+}, which also had unusual UV spectra in the region of 290 nm; it did not quite coincide to that observed for known G-quadruplex structures (38). Therefore, it is not clear whether TRF2^B induces T7-all to form a G-quadruplex structure.

TRF2^B does not promote parallel-stranded structures in Na^+

Oligonucleotides of human telomeric sequence typically form antiparallel-stranded structures in Na^+ (32). As expected, in the presence of 15 mM Na_2PO_4, T4, T7 and T8 show spectra typical of antiparallel G-quadruplexes, each having a peak at ~295 nm, a negative peak at ~265 nm and a smaller positive peak at ~245 nm (Figure 2A). The addition of TRF2^B to these did not significantly change the spectra, suggesting that induction of

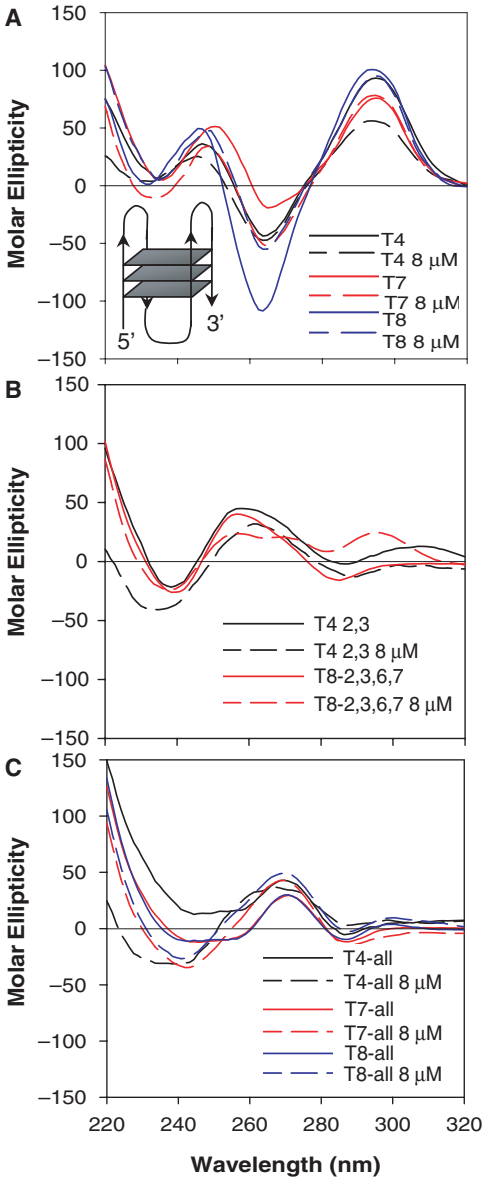

Figure 2. CD spectra exhibiting the effects of TRF2^B (0 or 8 μM) on 4 μM telomeric sequences T4, T8 (**A**), T4-2,3, T8-2,3,6,7 (**B**), T4-all and T8-all (**C**) in 15 mM Na_2PO_4. Samples were treated as in Figure 1. Molar ellipticity is in deg cm^2/dmol of bases. Inset in (A) represents an example of one type of antiparallel, intramolecular G-quadruplex formed by T4.

parallel-stranded structures by TRF2^B requires the presence of K^+.

The spectra for T4-2,3, T8-2,3,6,7, T4-all, T7-all and T8-all in 15 mM Na_2PO_4 were similar to the corresponding spectra for these oligonucleotides in 1 mM Na_2PO_4 (Figure 2B, 2C and data not shown), indicating that these oligonucleotides do not form G-quadruplex structures in Na^+. Furthermore, addition of the TRF2^B did not alter the spectra. Although these results were expected for T4-all, T7-all and T8-all, it was possible that T4-2,3 and T8-2,3,6,7 might form at least antiparallel structures in Na^+, with the assistance of TRF2^B. However, these results raise the possibility that T4-2,3 and T8-2,3,6,7 only form parallel-stranded structures which, as we have shown (31,38), require a different cation (e.g. K^+ or Sr^{2+}).

TRF2^B affects G-quadruplex structures in a time-dependent manner

Previous work (31,34) suggested that T7 is capable of forming both intramolecular and intermolecular quadruplex structures in K^+. T7 was shown to form a parallel/antiparallel-stranded, intramolecular G-quadruplex structure during short incubation periods in K^+ (31). Native gel electrophoresis and CD measurements showed that heating followed by slow cooling resulted in the formation of a mixture of intra and intermolecular structures with evidence of a greater population of parallel-stranded structures compared to fast cooling (31). To determine the effect of the TRF2^B on the time-dependent formation of certain G-quadruplex structures, the CD spectra for T7 or T8 with or without TRF2^B were measured at various time points between 0 and 24 h. As described in the last sections, the samples were heated and cooled quickly before the addition of the TRF2^B. The spectrum of T7 in 15 mM Na_2PO_4, 100 mM K^+ changed over time (Figure 3A) as expected from previous work. Initial time points (<1 h) resulted in the appearance of a large peak at 290 nm and a broad shoulder at 250–270, indicative of a mixed population of structures. Previous work suggested that the ~250 nm signal for this oligonucleotide could be attributed to non-quadruplex structures, while signals at 270 and 290 indicated an intramolecular G-quadruplex [(31) and data not shown]. The presence of TRF2^B for <1 h, resulted in a stronger signal at 265 nm suggesting an increase in the amount of G-quadruplex structures with an increase in parallel-stranded character. In the absence of TRF2^B, the signal at 4 h still displayed a broad shoulder at 250–270, although by 8 h of incubation the signal at 265 nm approached the amplitude of that at 290 nm and did not significantly change with further incubation. A 4 h incubation with TRF2^B increased the signal at 265 nm resulting in a bimodal spectra with two nearly equivalent-sized peaks at 265 nm and 290 nm. The signal at 265 continued to increase relative to the 290 nm peak with incubation of T7 with TRF2^B for 8–24 h. This demonstrates that the parallel-stranded structures formed in the presence of TRF2^B and K^+, assemble slower than parallel/antiparallel-stranded structures.

T8, as two-tandem T4 units, forms intramolecular G-quadruplex structures. These structures form quickly,

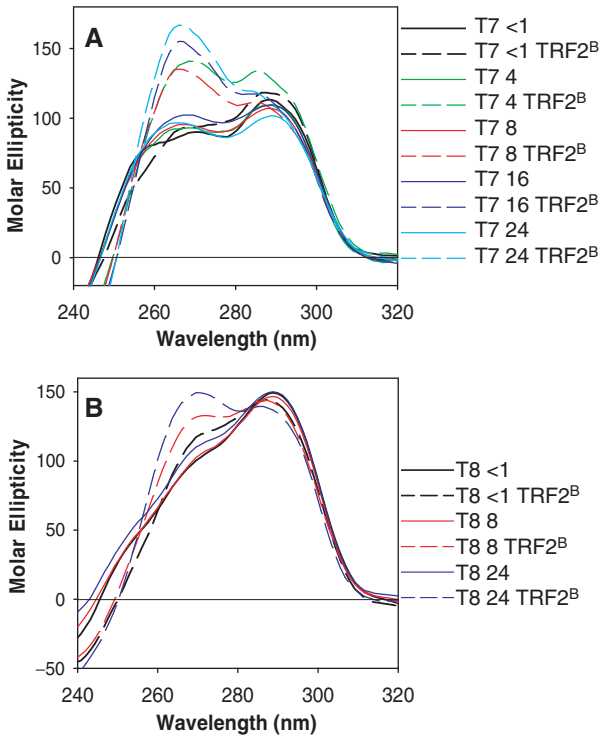

Figure 3. Time-dependent changes in the CD spectra of T7 (**A**) and T8 (**B**) $(TTAGGG)_{7 \text{ or } 8}$ (4 μM) with TRF2^B (8 μM) for <1* to 24 h in 15 mM Na_2PO_4 and 100 mM KCl. Samples were treated as in Figures 1 and 2, except that CD measurements were taken after incubation for the hours indicated by the numbers adjacent to oligonucleotide in spectra key. *<1 h refers to addition of TRF2^B and immediate acquisition of spectra (elapsed time ~30 min). Molar ellipticity is in deg cm^2/dmol of bases. Only signals obtained within wavelengths 220–320 nm and molar ellipticities −50 to +150 were displayed, to emphasize the time-dependent changes in this region of the spectra.

in less than an hour, and are not greatly affected by time or annealing conditions. Without TRF2^B, there was little change in T8 CD spectra from 1–24 h incubation times in 15 mM Na_2PO_4, 100 mM K^+ (Figure 3B), nor was there a large difference between slow-cooled (31) and quick-cooled samples. However, the addition of TRF2^B to T8 in K^+ resulted in a time-dependent increase in amplitude of the signal at 265 nm (Figure 3B), transitioning from an initial shoulder to a stronger signal slightly larger than the amplitude of the peak at 290 nm in the absence of TRF2^B. However, the ratio of 265 nm to 290 nm signals for T8 at 24 h was not as large as that observed with T7.

TRF2^B affects telomeric oligonucleotide electrophoretic mobility

To observe changes in mobility induced by the N-terminal basic domain of TRF2, 0–16 μM of TRF2^B was added to 4 μM of 5′-[^{32}P]-labeled telomeric oligonucleotides. In previous mobility shift assays (31), structures were allowed to form during a slow cooling and overnight incubation before loading onto gels. Those experimental conditions allowed for the appearance of slow-forming intermolecular structures. In these experiments, samples were heated

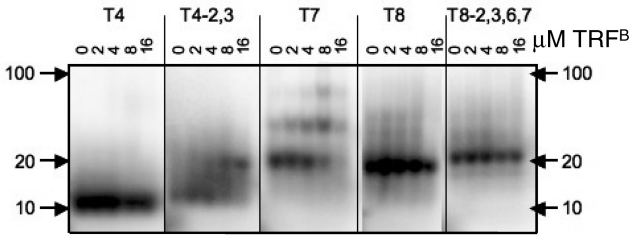

Figure 4. The effect of increasing concentrations of TRF2^B on the mobility of telomeric oligonucleotides. 5′-[^{32}P]-labeled oligonucleotides were treated as in Figures 1 and 2 before electrophoresis in 8% native polyacrylamide gels. TRF2^B concentration ranged from 0–16 μM, as indicated. Oligonucleotide concentrations were 4 μM. Molecular weight marker (M) sizes (10, 20, 100 bp) are indicated on the sides of the panel.

and immediately transferred to room temperature as was done for the CD obtained throughout this work.

The oligonucleotide T4-2,3 typically formed an intermolecular structure when subjected to gradual cooling in the presence of K^+, but was unable to form such a structure under rapid-cooling conditions (Figure 4). However, the addition of TRF2^B to T4-2,3 in K^+, resulted in the appearance of a slower-moving species, which had the same mobility as the previously identified intermolecular structure formed by slow cooling (31). It is important to note that these structures were only detected when K^+ was also present in polyacrylamide gels and running buffer, suggesting that these structures are K^+-stabilized G-quadruplexes. This shift was dependent on the concentration of TRF2^B, suggesting that TRF2^B may overcome the limitations of rapid-cooling and facilitate the assembly of an intermolecular structure.

In earlier studies (31,34), T7 was shown to form both a compact intramolecular G-quadruplex and an intermolecular structure. With the rapid cooling of this experiment, the majority of T7 remained in the intramolecular population. However, the addition of TRF2^B facilitated the formation of the intermolecular structures (Figure 4). Interestingly, 8 μM TRF2^B induced the appearance of a third band that had not been previously observed. By 16 μM TRF2^B concentration, most of intramolecular structure was converted into structures with slower mobilities. Thus, as with T4-2,3, TRF2^B appears to stimulate the formation of T7 intermolecular structures. Finally, TRF2^B (8 μM) stimulated only a small amount of intermolecular structures under dilute T7 concentrations (50 nM, data not shown).

The oligonucleotides T4, T8 and T8-2,3,6,7 were shown to form predominantly intramolecular G-quadruplexes in the presence of K^+ (31). Increasing amounts of TRF2^B did not significantly change the mobility of these oligonucleotides (Figure 4). These results, in combination with those in Figure 1, suggest that T4, T8 and T8-2,3,6,7 form intramolecular structures with parallel strand orientations. As expected, T4-all and T8-all, previously shown not to form G-quadruplex structures in K^+, showed no change in mobility with respect to TRF2^B concentration. These results suggest that in K^+, TRF2^B only stimulates intermolecular structures on oligonucleotides capable of forming them in K^+ under slow-cooling conditions. Taken together, the cation-dependence, oligonucleotide sequence-dependence, and similar electrophoretic mobilities to those observed in previous work suggest that TRF2^B stimulates the formation of parallel-stranded, and in some cases, intermolecular G-quadruplex structures.

Assimilation of a single-stranded telomeric oligonucleotide into telomeric plasmid DNA is less efficient in K^+ than in Mg^{2+} or Na^+

Uptake of a single-stranded telomeric oligonucleotide by a double-stranded plasmid containing telomeric DNA, has been observed either in the presence of crude cellular extracts (39), TRF2, or a truncated version of TRF2 containing the TRFH domain along with either the N-terminal or C-terminal nucleic-acid-binding domain (17). Factors in the cellular extracts may catalyze a strand-invasion reaction resulting in a displacement- or d-loop, which is one of the possible mechanisms for t-loop formation. However, the mechanism by which a plasmid can interact with a telomeric single-stranded oligonucleotide in the absence of proteins or extract, is more difficult to explain. Uptake only occurs when the plasmid has telomeric DNA, and the process is stimulated by the addition of Na^+ (17). Optimal single-strand oligonucleotide uptake requires TRF2 constructs containing the TRFH domain. This domain may alter DNA topology within the plasmid, and it may destabilize plasmid duplex DNA, providing an opportunity for annealing of the telomeric oligonucleotide (17). This reaction is more complicated than simple complementary base-pair annealing because the destabilization of the plasmid duplex may be facilitated by the formation of competing G-quadruplexes on the liberated regions of the plasmid G-strand. The formation of G-quadruplex structures either in the plasmid, in the oligonucleotide, or between the plasmid and oligonucleotide, may alter the uptake of single-stranded oligonucleotides, thus potentially having a role in t-loop formation.

To test how G-quadruplexes affected strand assimilation, 5′-[^{32}P]-labeled T7 oligonucleotide and pRST5, a ~96 TTAGGG repeat-containing plasmid (14), were combined under various reaction conditions. T7 was either heated just prior to its addition, to prevent preforming G-quadruplexes, or it was preincubated in salt, to promote structure formation. pRST5 was preincubated in Na^+, K^+ and/or Mg^{2+} before the reactions were combined and incubated at room temperature for 15 min or 24 h. The general trends described throughout this section were consistent regardless of preincubation conditions. As shown in previous figures, these conditions should result in the T7 oligonucleotide forming antiparallel quadruplexes in Na^+ and hybrid-type, parallel/antiparallel-stranded quadruplexes in K^+. In contrast, Mg^{2+} is expected to favor Watson–Crick duplexes over G-quadruplexes (40). Oligonucleotide uptake by the plasmid was stimulated by addition of either Mg^{2+} or Na^+, but higher concentrations of K^+ slightly inhibited the reaction (Figures 5A–D). Interestingly, the addition of K^+,

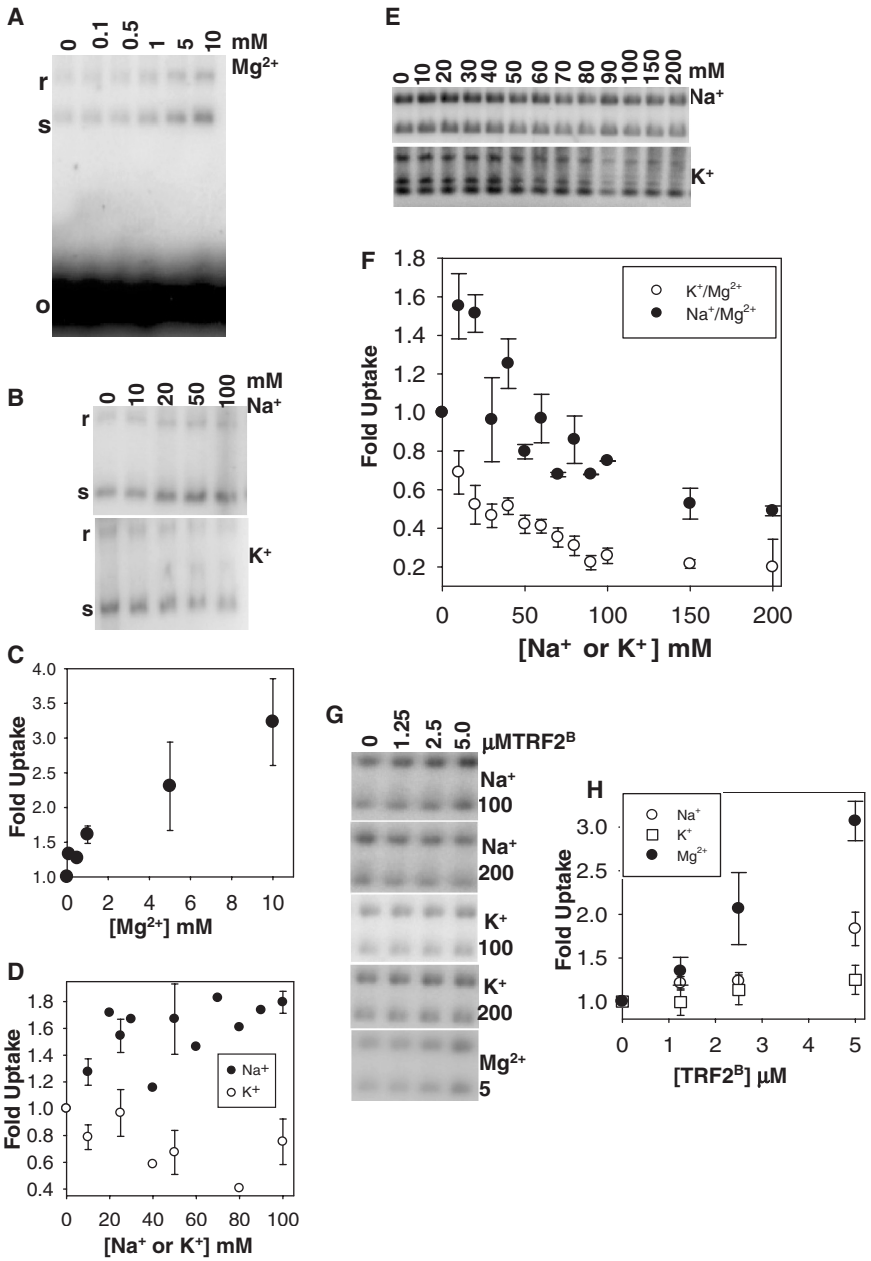

Figure 5. Uptake of T7 oligonucleotide into a telomeric plasmid. Single strand uptake assay with 50 nM 5′-[^{32}P]-labeled T7 oligonucleotide and unlabeled 20 ng/μl of pRST5 plasmid in indicated amounts of $MgCl_2$ (**A**), NaCl (**B**, top), or KCl (B, bottom) panel. Plasmid was preincubated in reaction buffer with appropriate salts. Oligonucleotide was heated for 5 min at 95°C and cooled overnight to room temperature before adding to the reactions. Reactions were incubated overnight at room temperature. Samples were electrophoresed on 1% agarose gels. o, s and r on the sides of the gels refer to free oligonucleotide (o) and oligonucleotide incorporated into relaxed (r) and supercoiled (s) pRST5 for A only. The rest of the gels only show (r) and (s) bands. Plots (**C**) and (**D**) correspond to experiments represented in A and B, respectively. Error represents 1 SD of the mean. Agarose gels (**E**) of T7 uptake in 5 mM $MgCl_2$ and indicated amounts of NaCl (top panel) or KCl (bottom panel). Plot (**F**) of experiments represented E. Agarose gels (**G**) of T7 uptake and indicated amounts of $TRF2^B$ in salts (mM) specified on the sides of gels. Reactions were incubated for 24 h at room temperature. Plot (**H**) of quantification of experiments in 5 mM Mg^{2+}, 100 mM Na^+ or K^+ represented in G.

which would stabilize G-quadruplex structures, to reactions containing 5 mM Mg^{2+} significantly inhibited the reaction (Figure 5E and F). Furthermore, electrophoresis of reaction products in agarose or native polyacrylamide gels in the presence of K^+, to stabilize possible intermolecular G-quadruplexes formed between the plasmid and T7 oligonucleotide, did not increase the amount of T7 bound to the plasmid (data not shown). Therefore, our results suggest that G-quadruplex formation is not necessary for uptake of T7 by the plasmid, and G-quadruplexes formed in the presence of K^+ partially inhibit the reaction under the conditions of the experiment. In fact, T4, shown to form more stable G-quadruplexes in K^+, was still assimilated into the plasmid in either Na^+ or K^+, albeit even less efficiently than T7 (data not shown).

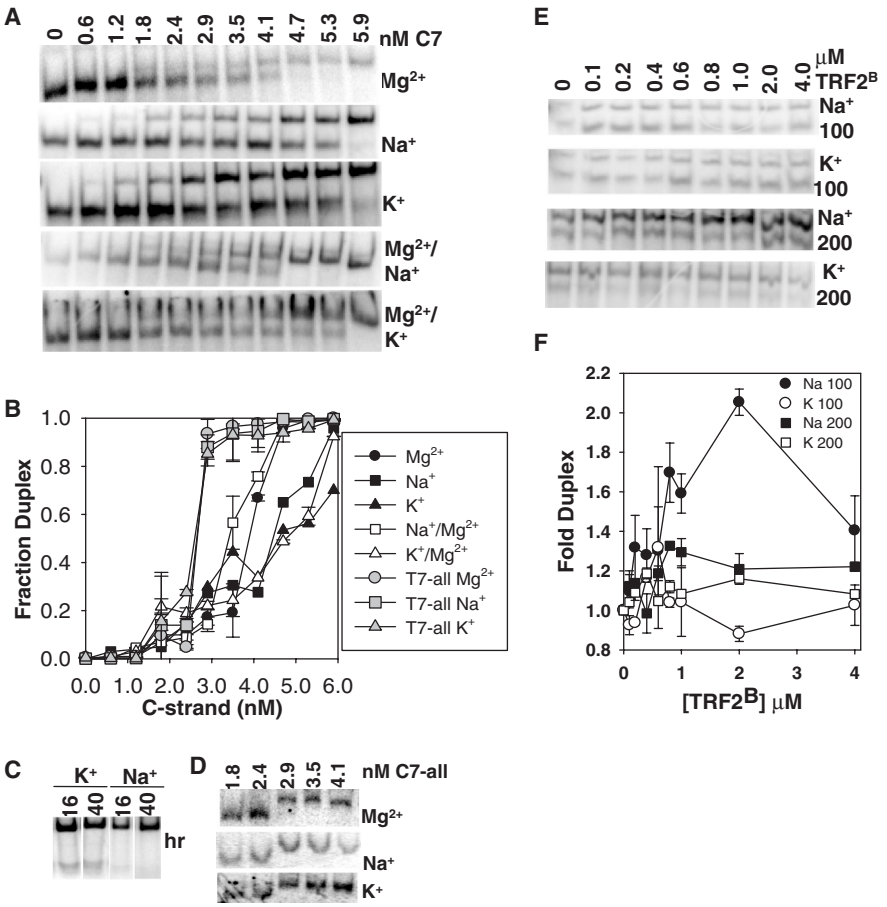

Figure 6. Salt-dependent annealing of T7 oligonucleotide to its complementary strand. Native polyacrylamide gels (**A**) of 5′-[^{32}P]-labeled T7 oligonucleotide (2.2 nM) incubated with indicated amounts of C7 [5′-d(CCCTAA)$_7$-3′] in salts (5 mM $MgCl_2$, 200 mM NaCl, 200 mM KCl or combination) indicated on sides of gels. Plots of fraction of duplex (duplex/total T7) (**B**) with increasing C7 or C7-all concentrations from gels represented in A and D. Extended incubation at indicated times (16 or 40 h) in 200 mM NaCl or KCl (**C**). Gels of T7-all (2.1 nM) annealing to indicated amounts of C7-all [5′-d(CTCTAA)$_7$-3′] strand (**D**) in salts (5 mM Mg^{2+}, 200 mM Na^+ or K^+) as specified on sides of gels. Effect of designated TRF2^B concentrations on the annealing of T7 (2.5 nM) to C7 (2.0 nM) in 100 or 200 mM salts as specified (**E**). Plot of quantification (**F**) of gels in E as fold duplex (fraction duplex as a function of TRF2^B normalized to fraction duplex at 0 nM TRF2^B).

The addition of TRF2^B further stimulated T7 uptake by pRST5 (Figure 5G and H) in the presence of Mg^{2+}. TRF2^B also stimulated T7 uptake in the presence of 50 mM K^+ or Na^+ (data not shown). However, TRF2^B-stimulated uptake of T7 was reduced in 100 mM Na^+ and eliminated in 100 mM K^+ (Figure G and H). Finally, no stimulation of T7 uptake by TRF2^B was observed in 200 mM Na^+ or K^+ (Figure G). In all cases, T7 uptake by pRST5 was less efficient in K^+ than in either Mg^{2+} or Na^+, and TRF2^B did not overcome this effect.

Competition between G-quadruplex and Watson–Crick duplex DNA

To better understand the results of the single-strand uptake assay, formation of Watson–Crick duplex DNA was directly tested under similar conditions as those of the single-strand uptake assay. In dilute oligonucleotide conditions, it is thought that intramolecular G-quadruplex structures affect the amount of guanine-rich strand available for annealing to its complementary strand in the presence of K^+ (41). Here, T7 samples were preheated in the respective salts to 95°C and slowly cooled over an hour to room temperature to form G-quadruplexes. Increasing concentrations of the complementary strand (C7) was added, and the reaction was incubated for an additional 15 min (or additional indicated times) before electrophoresis in native polyacrylamide gels containing the appropriate salt. In 5 mM Mg^{2+}, a cooperative transition to duplex DNA occurred requiring 3.9 nM C-strand for 50% of the G-strand to be in duplex form (Figure 6A and B). The transition in 200 mM Na^+ was slightly less cooperative, and more C-strand was required for 50% pairing than in Mg^{2+}. Meanwhile, the C-strand titration with both 5 mM Mg^{2+} and 200 mM Na^+ was more similar to that of Mg^{2+} alone. The titration in K^+ was similar to that of Na^+. However, unlike that observed with Na^+, addition of 5 mM Mg^{2+} to the K^+ reaction had less effect on the titration curve. In addition, longer incubation times (up to 16 and 40 h) of a 1:1 ratio of G-strand with C-strand in K^+, showed that ~5–10% of the G-strand was still resistant to annealing to C-strand (Figure 6C).

Under the same conditions in Na^+, nearly 100% of the G-strand was annealed to the C-strand.

The altered telomeric sequence, T7-all, was used as a control to determine if the salt-dependent effects were due to a competing structure in the G-strand, such as the G-quadruplex. The curves for all three salts were much more similar with this oligonucleotide pair than with T7 and C7 (Figure 6D and B). These results, together with the findings that annealing of T7 to C7 was least efficient in K^+, suggest that G-quadruplexes can inhibit duplex formation at these oligonucleotide concentrations. However, it is important to note that long incubation times resulted in only 5–10% of oligonucleotide being resistant to annealing to the complementary strand, suggesting that even in dilute oligonucleotide conditions, T7-C7 duplex is largely favored over G-quadruplex structures.

The TRFH domain stimulates strand-assimilation and intermolecular G-quadruplexes but does not promote parallel-stranded structures

Earlier studies showed that the TRF2 TRFH domain was crucial for optimal oligonucleotide uptake by a telomeric DNA plasmid (17). To determine the role of the TRFH domain in oligonucleotide uptake under G-quadruplex-promoting conditions, we analyzed both full-length TRF2 and a construct containing amino acids 3–247 of TRF2 ($TRF2^{BH}$) that comprises both the basic region and TRFH domain, in the oligonucleotide uptake assay. Like the basic region ($TRF2^{B}$), TRF2 and $TRF2^{BH}$ stimulated T7 uptake (Figure 7A and B) in the presence of Na^+. In agreement with earlier findings (17), TRF2 stimulated more T7 uptake than $TRF2^{BH}$ and both were more efficient than $TRF2^{B}$. Unlike that observed with the $TRF2^{B}$, lower concentrations of TRF2 and $TRF2^{BH}$ stimulated T7 uptake in K^+. This suggests that the presence of the TRFH domain was required for optimal, TRF2-dependent T7 uptake in K^+. However, higher concentrations of TRF2 partially reversed the stimulation observed at lower concentrations and higher concentrations of $TRF2^{BH}$ inhibited the reaction.

The T7 uptake results may reflect the ability of $TRF2^{BH}$ to promote G-quadruplexes under certain conditions. The TRFH domain of TRF2 is a homodimerization domain. Therefore, it is possible that homodimers containing the N-terminal DNA-binding region would stimulate the formation of intermolecular G-quadruplexes by bringing together separate oligonucleotide strands. This is particularly important under dilute oligonucleotide concentrations in which less K^+-induced, intermolecular G-quadruplexes form. Indeed, an 8-h incubation of $TRF2^{BH}$ with 50 nM T7 (80-fold more dilute than experiments in Figures 1–4) in K^+ stimulated the formation of slower-migrating structures in a $TRF2^{BH}$-concentration-dependent manner (Figure 7C and D). More of these structures formed at 24 h incubation times. In contrast to that observed with the basic region ($TRF2^{B}$) alone (Figure 4), $TRF2^{BH}$ did not induce substantial intermolecular structures with the T4-2,3 oligonucleotide (Figure 7C and D). As in Figure 4, these structures had similar mobilities to those observed previously (31) and required K^+ in the gels and running buffer.

To further ascertain whether $TRF2^{BH}$ affects parallel-stranded G-quadruplex formation, CD was performed. As expected, $TRF2^{BH}$ had a spectrum in the far UV indicative of its known alpha-helical structure (Figure 7F). Unlike that observed in the presence of $TRF2^{B}$, $TRF2^{BH}$ did not increase the amount of G-quadruplex character for T7 at short (<1 h) incubation times (Figure 7E). Moreover, very little increase in parallel-stranded G-quadruplexes was induced by $TRF2^{BH}$ at 24 h. Due to the limits of CD analysis, we were unable to evaluate the structures formed at 50 nM DNA concentrations for G-quadruplex character, but their mobilities were similar to those of the structures formed at higher DNA concentrations (data not shown), which we have analyzed by CD. Taken together, the results suggest that the presence of the TRFH domain facilitates the ability of the basic region to stimulate intermolecular structures on the T7, but not the T4-2,3 oligonucleotide. However, while it seems to facilitate some intermolecular structure formation like $TRF2^{B}$ alone, the TRFH domain appears to inhibit the parallel strand-inducing activity of the basic region.

DISCUSSION

Due to the ability to form Hoogsteen-like bonds, guanine-rich DNA has been shown to form a variety of non-Watson–Crick structures, including G-quadruplexes. Extensive characterization on the stability, kinetics and types of quadruplex formation under certain conditions, demonstrates the likelihood of the formation of these structures in certain regions of the genome, particularly at times when guanine-rich sequences may be isolated from their complementary strands. An example of this is the G-strand overhang of telomeres. However, G-quadruplex structures, even at the G-strand overhang, may compete with the complementary strand in the t-loop model or be destabilized by single-stranded DNA-binding proteins such as POT1 (42,43). This article describes the first study characterizing the effects of the nucleic acid-binding region in the N-terminus of TRF2 on the formation of G-quadruplexes.

Our mobility and CD data show that $TRF2^{B}$ stimulated the formation of parallel-stranded and intermolecular structures, but only in the presence of K^+, not Na^+. Although CD and gel analysis are indirect methods for determining structure, the cation and sequence specificity for the results obtained in this study are consistent with these structures being G-quadruplexes. The cation-specific findings are important since physiological concentrations are typically higher in K^+ than Na^+ stressing the possibility that TRF2 can modulate the structure of G-quadruplexes in the cell.

This study also shows that substantial intermolecular structure formation required micromolar oligonucleotide concentrations and could only form with oligonucleotides previously shown to form intermolecular structures. We have shown that these intermolecular structures form over

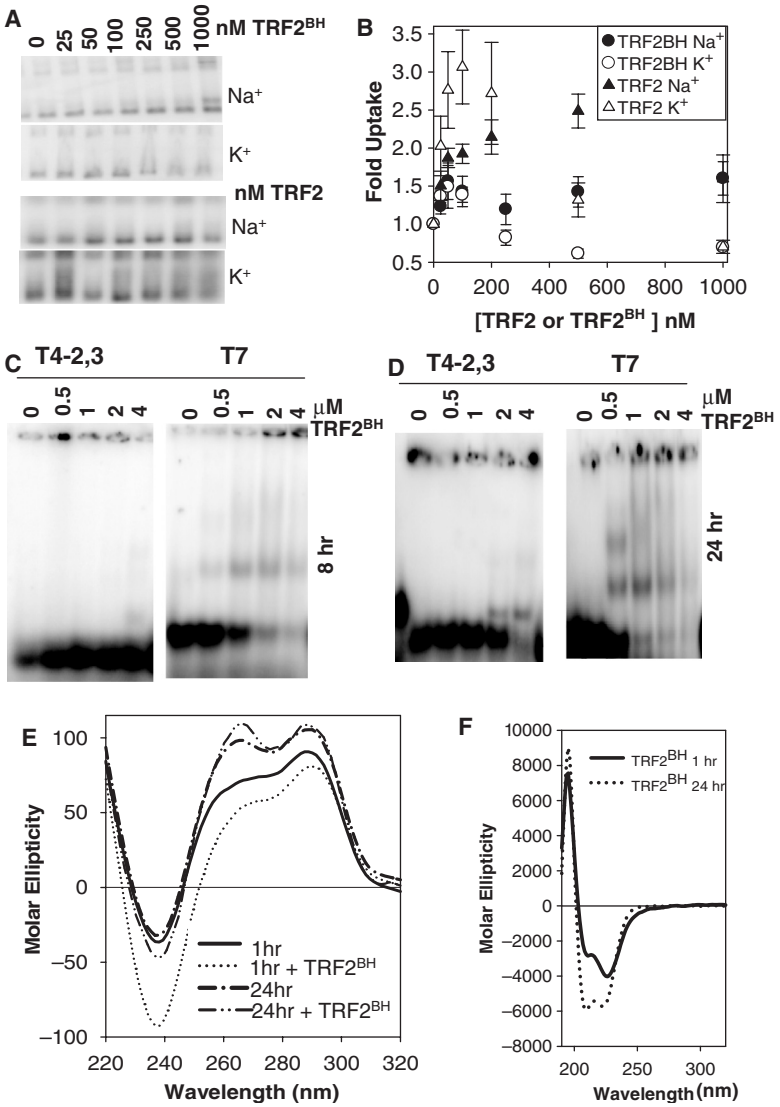

Figure 7. Effects of $TRF2^{BH}$ on G-quadruplex structures and T7 uptake by pRST5. Effect of $TRF2^{BH}$ (top two panels) and TRF2 (bottom two panels) on the uptake of T7 oligonucleotide by pRST5 (**A**). Experiments performed with indicated amounts of $TRF2^{BH}$ or TRF2 and salts (100 mM) as described in Figure 5. Plots (**B**) of quantification of gels represented in (A). $TRF2^{BH}$ binding alters the mobility of telomeric G-quadruplex structures (**C** and **D**). Reactions with 50 nM 5′-[^{32}P]-labeled T7 in 100 mM KCl, 22.5 mM NaCl and $TRF2^{BH}$ treated according to Materials and Methods before electrophoresis on 12% native polyacrylamide gels. T7 with $TRF2^{BH}$ were incubated for 8 (C) or 24 (D) h. CD spectra (**E**) of $TRF2^{BH}$ (2 μM) with T7 (2 μM) in 100 mM KF, 12.5 mM NaCl and 1 mM Na_2PO_4. Samples were treated as in Figure 1. Molar ellipticity is in deg cm^2/dmol of bases. CD spectra (**F**) of $TRF2^{BH}$ alone in 100 mM KF, 12.5 mM NaCl and 15 mM Na_2PO_4 at indicated times. Molar ellipticity is in deg cm^2/dmol of amino-acid residues.

the course of several hours (31). In addition, recent studies (44,45) demonstrate that human telomeric DNA initially forms antiparallel structures in a path toward final structures with more parallel-strand or parallel/antiparallel strand orientation, suggesting that parallel-stranded G-quadruplexes also form more slowly. Our results confirm this. T7 has a T4 unit capable of forming an intramolecular G-quadruplex, with hybrid-type, parallel/antiparallel strand orientation, attached to a T3 unit shown to form intermolecular structures. Heating and slow cooling resulted in a population divided between unimolecular and intermolecular structures (31,34). In addition, the amount of parallel strand orientation in these structures increased over time (31), suggesting that parallel-stranded quadruplex with human telomeric sequences have slower rates of formation. The work in this study also shows that $TRF2^{B}$ stimulated the rate and amount of parallel-stranded, intermolecular structures for T7. The addition of equimolar amounts of $TRF2^{B}$ resulted in a slight increase in the parallel-stranded character of the population with an increase in the amplitude of the CD spectrum near 265 nm. Doubling the amount of $TRF2^{B}$ in the reaction caused a dramatic increase in the peak near 265 nm of the CD spectrum, suggesting that the $TRF2^{B}$ stabilizes parallel-quadruplexes in a concentration-dependent manner. Interestingly, this increase in amplitude was not accompanied by a decrease in the molar ellipticity near 290 nm. These spectral

transitions may be explained in the context of results from native gel electrophoresis (Figure 4). Addition of increasing amounts of $TRF2^{B}$ promotes the formation of increasingly higher-order structures. Taken together, these results suggest that $TRF2^{B}$ stimulates the formation of intermolecular and parallel-stranded G-quadruplex structures. These could be concurrent or additive events. Our experiments cannot separate whether the whole population is shifting towards more parallel-stranded character or if the intramolecular structures remain the same while $TRF2^{B}$ stimulates *de novo* parallel, intermolecular G-quadruplexes from non-quadruplex structures in the population.

Similarly, heating and slowly cooling T4-2,3 in K^+ forms an intermolecular structure with a CD spectrum that suggests exclusively parallel strand orientation if it is a G-quadruplex (Figures 1 and 4). $TRF2^{B}$ stimulates this structure under fast-cooling conditions. Unlike T4, T4-2,3 cannot form intramolecular G-quadruplexes under fast-cooling conditions because the required central guanine in the second and third 5′-dTTAGGG-3′ repeats are altered. Although T8-2,3,6,7 can form intramolecular structures with slow cooling, it requires the presence of $TRF2^{B}$ to form a parallel-stranded structure when fast cooled. In this way, T4-2,3 and T8-2,3,6,7 are very similar and the results further support the concept that parallel-stranded G-quadruplexes form more slowly but are facilitated by $TRF2^{B}$.

$TRF2^{B}$ also converted the CD spectra of T4 and T8 from more hybrid, parallel/antiparallel-stranded G-quadruplexes to those suggesting more parallel-strand orientation (Figure 1). Again, the rate of parallel-strand structure formation was slow compared to the hybrid-strand structure (Figure 3). In contrast to T7 and T4-2,3, the mobility of T4 and T8 in the native gels were not significantly changed by $TRF2^{B}$ (Figure 4), suggesting that these represent intramolecularly folded G-quadruplexes with propeller-like loops (Figure 1G) (46).

Some aspects of these results are similar to those obtained for these and other telomeric oligonucleotides in the presence of Sr^{2+} and Ca^{2+} (38,47). In addition, molecular crowding conditions, such as 2 M PEG, favored parallel-stranded structures for the 5′-d(G4T4G4) GTG-3′ in Na^+, most likely through an excluded volume mechanism since PEG was not shown to strongly interact with the oligonucleotides (30,35). This suggests that crowding may serve to switch conformations between types of G-quadruplexes. Interestingly, various polyamines (30) and polylysine (48) have been shown to interact with these oligonucleotides without converting the G-quadruplex antiparallel strand orientation in Na^+. This is in agreement with our findings in Na^+.

Together, our results suggest that the N-terminus of TRF2 acts as a polycation by promoting the intrinsic ability of telomeric DNA to form certain G-quadruplex structures. This concept is supported by preliminary data showing that rearrangement of two of the eight arginines within $TRF2^{B}$ (data not shown), did not impair the ability to facilitate the formation of intermolecular G-quadruplexes. Additional studies are required to determine the specificity of the N-terminal region for promoting certain G-quadruplex structures. However, this region is conserved in mammals and an earlier study showed that rearrangement of just two arginines diminished the ability of an N-terminal peptide to recognize four-way junction DNA (13). It was suggested that this DNA structure-specific recognition had a role in preventing XRCC3-dependent telomere loss to extrachromosomal circles observed in cells expressing a $TRF2^{\triangle B}$ mutant (16).

Interestingly, the properties of $TRF2^{BH}$ were distinct from $TRF2^{B}$. It was expected that the homodimerization domain may increase interactions with the oligonucleotides and facilitate intermolecular interactions. Indeed, lower concentrations of $TRF2^{BH}$ than $TRF2^{B}$ were required to stimulate intermolecular complex formation (Figures 4 and 7). Moreover, $TRF2^{BH}$ was capable of stimulating intermolecular structures with more dilute oligonucleotide concentrations than that observed with $TRF2^{B}$. However, $TRF2^{BH}$ did not appear to stimulate parallel-stranded G-quadruplex formation and did not stimulate intermolecular structures with T4-2,3. The reasons for these differences are unclear if it is assumed that the basic region is the nucleic-acid-binding region and that the TRFH domain simply acts as a homodimerization domain. Nevertheless, the different effects of the $TRF2^{B}$ and $TRF2^{BH}$ extend beyond their affects on the type of G-quadruplexes formed.

$TRF2^{B}$ and $TRF2^{BH}$ have slightly different activities in the single strand uptake assay. Several factors can influence this reaction. Amiard *et al.* (17) suggested that TRF2 increases the superhelical density, thus destabilizing duplex DNA to allow for annealing of a telomeric oligonucleotide. This reaction occurs with less efficiency in the absence of TRF2 and is stimulated by Na^+. This apparent fluidity in telomeric DNA was also observed when artificial telomeric replication forks spontaneously reverted to 'chicken foot' structures *in vitro* (49). One possible explanation for the dynamic nature of telomeric DNA is the ability to form G-quadruplexes. However, our results show that assimilation of T7 into the telomeric plasmid is most strongly stimulated by Mg^{2+}, which forms weak G-quadruplexes and can actually destabilize preformed G-quadruplexes, when added at high concentrations to Na^+ solutions (40). This suggests that G-quadruplex formation within the plasmid is unnecessary for this reaction. Another factor in this reaction is the structure of the single strand to be taken up by the plasmid. Our results show that Na^+ stimulates single strand uptake but is less efficient than Mg^{2+}, as expected, for favoring Watson–Crick duplex formation between T7 and the plasmid. Single strand uptake was even less efficiently stimulated by K^+. The duplex annealing assay showed that the G-strand preincubated in K^+ was resistant to annealing to the C-strand; approximately 10% remained resistant for up to 40 h of incubation. Moreover, a combination of Mg^{2+} and Na^+ further stimulated duplex formation compared to Na^+ alone. This further stimulation with Mg^{2+} was not observed in the K^+ reaction. One explanation for this is that telomeric G-quadruplexes formed in K^+ may compete with duplex DNA and could potentially affect the formation of structures such as t-loops.

These results are consistent with other studies showing that a small but significant population of the guanine-rich strand will remain in the form of a G-quadruplex in the presence of the complementary strand (41). This is more pronounced in K^+ than Na^+.

Our results also show that $TRF2^B$ does not appear to greatly affect single strand assimilation into the telomeric plasmid in the presence of K^+ (Figure 5). Moreover, low concentrations of TRF2 and $TRF2^{BH}$ stimulated single-stranded oligonucleotide uptake even in reactions containing K^+ (Figure 7). This suggests that the TRFH domain of TRF2 may contribute to overcoming any G-quadruplex-dependent inhibition of annealing to C-strand even if the N-terminal basic region facilitates the formation of parallel-stranded structures. Moreover, the myb-like DNA-binding domain of TRF2 may further favor the duplex form of telomeric DNA by binding to the major groove (6), in agreement with results in Figure 7A showing that more T7 uptake was observed with addition of TRF2 than with $TRF2^{BH}$.

Since TRF2 and $TRF2^{BH}$ have the capability of overcoming the K^+-dependent inhibition of T7 uptake, it is tempting to speculate that G-quadruplexes have only a minor role in t-loop formation or duplex fluidity throughout telomeric DNA. However, it is important to note that many variables may bring these structures into play. The most important is the molecular crowding that may exist in the nucleus. Molecular crowding has been shown repeatedly to favor parallel-stranded G-quadruplexes for a variety of telomeric sequences, including human, and increases their melting temperatures (50,51). More importantly, crowding by PEG destabilizes duplex DNA while stabilizing parallel-stranded G-quadruplexes (52). It will be interesting to see if the presence of molecular crowders significantly alters the reactions described in this work. Furthermore, there are likely instances in which the G-strand is separate from the C-strand. For example, the C-strand may form an i-motif, a tetrad structure usually formed at lower pH than that of our reaction conditions (53). It is also not clear at this time whether all telomeres are in the form of t-loops. Telomeres not in t-loop form would end in a free G-strand overhang, which may be subject to the formation of G-quadruplexes and modulation by the TRF2 N-terminus. In this way, TRF2 may affect the activity of telomerase, particularly since telomerase from ciliates have recently been shown to preferentially act upon parallel-stranded, tetramolecular G-quadruplexes over intramolecular G-quadruplexes (22,23). TRF2 may even have different effects on shelterin stability around the single-strand/double-strand DNA junction. Transient free G-strand may also exist during replication, where RecQ helicases such as WRN, which unwind G-quadruplexes, are required for efficient lagging strand synthesis (54). Finally, small molecule telomerase inhibitors may shift the population toward G-quadruplex (55), although this may also disrupt TRF2 interactions (27). These examples stress the importance of studying how molecular crowding and nucleoproteins affect the structure of G-quadruplexes.

SUPPLEMENTARY DATA

Supplementary Data are available at NAR Online.

ACKNOWLEDGEMENTS

We thank Diana Azzam, Di Ding and Hassan Al-Ali for help in purification of $TRF2^{BH}$. We also thank the laboratory of Dr Thomas K. Harris for the use of the Akta FPLC and Dr James Potter for the use of his spectropolarimeter.

FUNDING

This work was supported by the James and Esther King, Florida Biomedical Research Program [04NAR-06] and the American Heart Association [07552813]. Funding for open access charge: American Heart Association [07552813].

Conflict of interest statement. None declared.

REFERENCES

1. Palm,W. and de Lange,T. (2008) How Shelterin Protects Mammalian Telomeres. *Annu. Rev. Genet.*, **42**, 301–334.
2. Von Zglinicki,T. (2003) Replicative senescence and the art of counting. *Exp. Gerontol.*, **38**, 1259–1264.
3. Cong,Y.S., Wright,W.E. and Shay,J.W. (2002) Human telomerase and its regulation. *Microbiol. Mol. Biol. Rev.*, **66**, 407–425.
4. Broccoli,D., Smogorzewska,A., Chong,L. and de Lange,T. (1997) Human telomeres contain two distinct Myb-related proteins, TRF1 and TRF2. *Nat. Genet.*, **17**, 231–235.
5. Bilaud,T., Brun,C., Ancelin,K., Koering,C.E., Laroche,T. and Gilson,E. (1997) Telomeric localization of TRF2, a novel human telobox protein. *Nat. Genet.*, **17**, 236–239.
6. Court,R., Chapman,L., Fairall,L. and Rhodes,D. (2005) How the human telomeric proteins TRF1 and TRF2 recognize telomeric DNA: a view from high-resolution crystal structures. *EMBO Rep.*, **6**, 39–45.
7. Baumann,P. and Cech,T.R. (2001) Pot1, the putative telomere end-binding protein in fission yeast and humans. *Science*, **292**, 1171–1175.
8. van Steensel,B., Smogorzewska,A. and de Lange,T. (1998) TRF2 protects human telomeres from end-to-end fusions. *Cell*, **92**, 401–413.
9. Karlseder,J., Broccoli,D., Dai,Y., Hardy,S. and de Lange,T. (1999) p53- and ATM-dependent apoptosis induced by telomeres lacking TRF2. *Science*, **283**, 1321–1325.
10. Griffith,J.D., Comeau,L., Rosenfield,S., Stansel,R.M., Bianchi,A., Moss,H. and de Lange,T. (1999) Mammalian telomeres end in a large duplex loop. *Cell*, **97**, 503–514.
11. Fairall,L., Chapman,L., Moss,H., de Lange,T. and Rhodes,D. (2001) Structure of the TRFH dimerization domain of the human telomeric proteins TRF1 and TRF2. *Mol. Cell*, **8**, 351–361.
12. Khan,S.J., Yanez,G., Seldeen,K., Wang,H., Lindsay,S.M. and Fletcher,T.M. (2007) Interactions of TRF2 with model telomeric ends. *Biochem. Biophys. Res. Commun.*, **363**, 44–50.
13. Fouche,N., Cesare,A.J., Willcox,S., Ozgur,S., Compton,S.A. and Griffith,J.D. (2006) The basic domain of TRF2 directs binding to DNA junctions irrespective of the presence of TTAGGG repeats. *J. Biol. Chem.*, **281**, 37486–37495.
14. Stansel,R.M., de Lange,T. and Griffith,J.D. (2001) T-loop assembly in vitro involves binding of TRF2 near the 3′ telomeric overhang. *EMBO J.*, **20**, 5532–5540.
15. Yoshimura,S.H., Maruyama,H., Ishikawa,F., Ohki,R. and Takeyasu,K. (2004) Molecular mechanisms of DNA end-loop formation by TRF2. *Genes Cells*, **9**, 205–218.

16. Wang,R.C., Smogorzewska,A. and de Lange,T. (2004) Homologous recombination generates T-loop-sized deletions at human telomeres. *Cell*, **119**, 355–368.
17. Amiard,S., Doudeau,M., Pinte,S., Poulet,A., Lenain,C., Faivre-Moskalenko,C., Angelov,D., Hug,N., Vindigni,A., Bouvet,P. *et al.* (2007) A topological mechanism for TRF2-enhanced strand invasion. *Nat. Struct. Mol. Biol.*, **14**, 147–154.
18. Burge,S., Parkinson,G.N., Hazel,P., Todd,A.K. and Neidle,S. (2006) Quadruplex DNA: sequence, topology and structure. *Nucleic Acids Res.*, **34**, 5402–5415.
19. Zahler,A.M., Williamson,J.R., Cech,T.R. and Prescott,D.M. (1991) Inhibition of telomerase by G-quartet DNA structures. *Nature*, **350**, 718–720.
20. Fletcher,T.M., Sun,D., Salazar,M. and Hurley,L.H. (1998) Effect of DNA secondary structure on human telomerase activity. *Biochemistry*, **37**, 5536–5541.
21. Sun,D., Lopez-Guajardo,C.C., Quada,J., Hurley,L.H. and Von Hoff,D.D. (1999) Regulation of catalytic activity and processivity of human telomerase. *Biochemistry*, **38**, 4037–4044.
22. Oganesian,L., Moon,I.K., Bryan,T.M. and Jarstfer,M.B. (2006) Extension of G-quadruplex DNA by ciliate telomerase. *EMBO J.*, **25**, 1148–1159.
23. Oganesian,L., Graham,M.E., Robinson,P.J. and Bryan,T.M. (2007) Telomerase recognizes G-quadruplex and linear DNA as distinct substrates. *Biochemistry*, **46**, 11279–11290.
24. Gunaratnam,M., Greciano,O., Martins,C., Reszka,A.P., Schultes,C.M., Morjani,H., Riou,J.F. and Neidle,S. (2007) Mechanism of acridine-based telomerase inhibition and telomere shortening. *Biochem. Pharmacol.*, **74**, 679–689.
25. Gomez,D., Paterski,R., Lemarteleur,T., Shin-Ya,K., Mergny,J.L. and Riou,J.F. (2004) Interaction of telomestatin with the telomeric single-strand overhang. *J. Biol. Chem.*, **279**, 41487–41494.
26. Gomez,D., O'Donohue,M.F., Wenner,T., Douarre,C., Macadre,J., Koebel,P., Giraud-Panis,M.J., Kaplan,H., Kolkes,A., Shin-ya,K. *et al.* (2006) The G-quadruplex ligand telomestatin inhibits POT1 binding to telomeric sequences in vitro and induces GFP-POT1 dissociation from telomeres in human cells. *Cancer Res.*, **66**, 6908–6912.
27. Tahara,H., Shin-Ya,K., Seimiya,H., Yamada,H., Tsuruo,T. and Ide,T. (2006) G-Quadruplex stabilization by telomestatin induces TRF2 protein dissociation from telomeres and anaphase bridge formation accompanied by loss of the 3′ telomeric overhang in cancer cells. *Oncogene*, **25**, 1955–1966.
28. Yanez,G.H., Khan,S.J., Locovei,A.M., Pedroso,I.M. and Fletcher,T.M. (2005) DNA structure-dependent recruitment of telomeric proteins to single-stranded/double-stranded DNA junctions. *Biochem. Biophys. Res. Commun.*, **328**, 49–56.
29. Fang,G. and Cech,T.R. (1993) Characterization of a G-quartet formation reaction promoted by the beta-subunit of the Oxytricha telomere-binding protein. *Biochemistry*, **32**, 11646–11657.
30. Miyoshi,D., Nakao,A. and Sugimoto,N. (2002) Molecular crowding regulates the structural switch of the DNA G-quadruplex. *Biochemistry*, **41**, 15017–15024.
31. Pedroso,I.M., Duarte,L.F., Yanez,G., Burkewitz,K. and Fletcher,T.M. (2007) Sequence specificity of inter- and intramolecular G-quadruplex formation by human telomeric DNA. *Biopolymers*, **87**, 74–84.
32. Balagurumoorthy,P. and Brahmachari,S.K. (1994) Structure and stability of human telomeric sequence. *J. Biol. Chem.*, **269**, 21858–21869.
33. Rujan,I.N., Meleney,J.C. and Bolton,P.H. (2005) Vertebrate telomere repeat DNAs favor external loop propeller quadruplex structures in the presence of high concentrations of potassium. *Nucleic Acids Res.*, **33**, 2022–2031.
34. Vorlickova,M., Chladkova,J., Kejnovska,I., Fialova,M. and Kypr,J. (2005) Guanine tetraplex topology of human telomere DNA is governed by the number of (TTAGGG) repeats. *Nucleic Acids Res.*, **33**, 5851–5860.
35. Yu,H.Q., Miyoshi,D. and Sugimoto,N. (2006) Characterization of structure and stability of long telomeric DNA G-quadruplexes. *J. Am. Chem. Soc.*, **128**, 15461–15468.
36. Dai,J., Carver,M., Punchihewa,C., Jones,R.A. and Yang,D. (2007) Structure of the Hybrid-2 type intramolecular human telomeric G-quadruplex in K+ solution: insights into structure polymorphism of the human telomeric sequence. *Nucleic Acids Res.*, **35**, 4927–4940.
37. Phan,A.T., Kuryavyi,V., Luu,K.N. and Patel,D.J. (2007) Structure of two intramolecular G-quadruplexes formed by natural human telomere sequences in K+ solution. *Nucleic Acids Res.*, **35**, 6517–6525.
38. Pedroso,I.M., Duarte,L.F., Yanez,G., Baker,A.M. and Fletcher,T.M. (2007) Induction of parallel human telomeric G-quadruplex structures by Sr(2+). *Biochem. Biophys. Res. Commun.*, **358**, 298–303.
39. Verdun,R.E. and Karlseder,J. (2006) The DNA damage machinery and homologous recombination pathway act consecutively to protect human telomeres. *Cell*, **127**, 709–720.
40. Li,W., Miyoshi,D., Nakano,S. and Sugimoto,N. (2003) Structural competition involving G-quadruplex DNA and its complement. *Biochemistry*, **42**, 11736–11744.
41. Zhao,Y., Kan,Z.Y., Zeng,Z.X., Hao,Y.H., Chen,H. and Tan,Z. (2004) Determining the folding and unfolding rate constants of nucleic acids by biosensor. Application to telomere G-quadruplex. *J. Am. Chem. Soc.*, **126**, 13255–13264.
42. Zaug,A.J., Podell,E.R. and Cech,T.R. (2005) Human POT1 disrupts telomeric G-quadruplexes allowing telomerase extension in vitro. *Proc. Natl Acad. Sci. USA*, **102**, 10864–10869.
43. Furukawa,A. and Torigoe,H. (2005) Tetraplex structure of fission yeast telomeric DNA and its unfolding by the interaction with telomeric DNA binding protein Pot1. *Nucleic Acids Symp. Ser.*, **49**, 63–64.
44. Gray,R.D. and Chaires,J.B. (2008) Kinetics and mechanism of K+- and Na+-induced folding of models of human telomeric DNA into G-quadruplex structures. *Nucleic Acids Res.*, **36**, 4191–4203.
45. Mashimo,T. and Sugiyama,H. (2007) Folding pathways of human telomeric hybrid G-quadruplex structure. *Nucleic Acids Symp. Ser.*, **51**, 239–240.
46. Parkinson,G.N., Lee,M.P. and Neidle,S. (2002) Crystal structure of parallel quadruplexes from human telomeric DNA. *Nature*, **417**, 876–880.
47. Miyoshi,D., Nakao,A. and Sugimoto,N. (2003) Structural transition from antiparallel to parallel G-quadruplex of d(G4T4G4) induced by Ca2+. *Nucleic Acids Res.*, **31**, 1156–1163.
48. Makita,N., Kano,A., Yamayoshi,A., Akaike,T. and Maruyama,A. (2005) Modulation of highly ordered structures of human telomeric sequence by cationic copolymers. *Nucleic Acids Symp. Ser.*, **49**, 53–54.
49. Fouche,N., Ozgur,S., Roy,D. and Griffith,J.D. (2006) Replication fork regression in repetitive DNAs. *Nucleic Acids Res.*, **34**, 6044–6050.
50. Karimata,H., Miyoshi,D. and Sugimoto,N. (2005) Structure and stability of DNA quadruplexes under molecular crowding conditions. *Nucleic Acids Symp. Ser.*, **49**, 239–240.
51. Miyoshi,D., Karimata,H. and Sugimoto,N. (2006) Factors regulating thermodynamic stability of DNA structures under molecular crowding conditions. *Nucleic Acids Symp Ser*, **50**, 203–204.
52. Kan,Z.Y., Lin,Y., Wang,F., Zhuang,X.Y., Zhao,Y., Pang,D.W., Hao,Y.H. and Tan,Z. (2007) G-quadruplex formation in human telomeric (TTAGGG)4 sequence with complementary strand in close vicinity under molecularly crowded condition. *Nucleic Acids Res.*, **35**, 3646–3653.
53. Phan,A.T. and Mergny,J.L. (2002) Human telomeric DNA: G-quadruplex, i-motif and Watson-Crick double helix. *Nucleic Acids Res.*, **30**, 4618–4625.
54. Crabbe,L., Verdun,R.E., Haggblom,C.I. and Karlseder,J. (2004) Defective telomere lagging strand synthesis in cells lacking WRN helicase activity. *Science*, **306**, 1951–1953.
55. Neidle,S. and Parkinson,G.N. (2008) Quadruplex DNA crystal structures and drug design. *Biochimie*, **90**, 1184–1196.